Downloaded from orbit.dtu.dk on: May 05, 2023

DTU Library

Nuclear accident dosimetry measurements at the 4th IAEA Intercomparison, Harwell, U.K., April 1975

Majborn, B.

Publication date:
1975

Document Version
Publisher's PDF, also known as Version of record

Link back to DTU Orbit

Citation (APA):
Majborn, B. (1975). *Nuclear accident dosimetry measurements at the 4th IAEA Intercomparison, Harwell, U.K., April 1975*. Risø National Laboratory. Risø-M No. 1830

General rights
Copyright and moral rights for the publications made accessible in the public portal are retained by the authors and/or other copyright owners and it is a condition of accessing publications that users recognise and abide by the legal requirements associated with these rights.

- Users may download and print one copy of any publication from the public portal for the purpose of private study or research.
- You may not further distribute the material or use it for any profit-making activity or commercial gain
- You may freely distribute the URL identifying the publication in the public portal

If you believe that this document breaches copyright please contact us providing details, and we will remove access to the work immediately and investigate your claim.

A. E. K. Risø

Risø - M - 1830

Risø - M - 1830

Title and author(s)

Nuclear Accident Dosimetry Measurements at the Fourth IAEA Intercomparison, Harwell, United Kingdom, April 1978.

Benny Majborn

Date November 1978

Department or group

Health Physics

Group's own registration number(s)

HP-78-143

9 pages + 9 tables + 4 illustrations

Abstract

Teams from several countries compared their systems for assessing doses in criticality accidents at the fourth IAEA intercomparison at Harwell. The dosimeters were exposed to mixed pulses of neutron and gamma radiation produced by the VYPER reactor at AWRE, Aldermaston.

Risø participated in the intercomparison experiment with the routine personnel dosimeters employed in "criticality areas" at Risø. These include the RKAEA criticality dosimeter for the measurement of neutron doses and the Risø TLD badge for the measurement of gamma doses.

The final results of the Risø measurements are presented in this report in a form designed for ease of comparison with those of other participants.

Copies to

**Available on request from the Library of the Danish Atomic Energy Commission (Atomenergikommissionens Bibliotek), Risø, DK-4000 Roskilde, Denmark
Telephone: (03) 35 51 01, ext. 334, telex: 43116**

ISBN 87-550-0625-3

ISBN 87 550 0366 4

CONTENTS

		page
1.	Introduction	1
2.	Irradiations	1
3.	Dosimeters used for the Risø measurements	2
4.	Measurement procedures	3
5.	Results	3
6.	Dose estimates	4
7.	Discussion	7
8.	Acknowledgements	8
9.	References	9
	Tables I - IX	
	Figures 1 - 4	

1. INTRODUCTION

Fifteen teams from twelve countries took part in the Fourth IAEA Intercomparison of Nuclear Accident Dosimetry Systems at Harwell, U.K., 7 - 15 April 1975. The performance of criticality dosimeters employed by the participating organisations was compared by simultaneous exposure of the dosimeters to pulsed radiation from the fast pulsed reactor VIPER at AWRE, Aldermaston. The Danish AEC Research Establishment Risø participated in the intercomparison experiment with the routine personnel dosimeters employed in areas classified as "criticality areas" at Risø.

The final results of the Risø measurements are presented in this report in a form designed for ease of comparison with those of other participants. At the time of writing the final results of other participants are not available. A summarizing report will be issued by the host institute.

2. IRRADIATIONS

The VIPER reactor (1,2,3) consists of a core of 37 % enriched uranium fuel pins in a matrix of aluminium-loaded epoxy resin and copper surrounded by a 20 cm thick copper reflector. The reactor can either produce a single fission burst or be operated at steady power for calibration measurements. In a normal full size pulse of 3.46×10^{17} fissions the power reaches a maximum of about 20,000 MW and the pulse has a full width at half maximum of 400 µs.

The dosimeters were irradiated at dosimetry stations situated along an arc of a circle of radius 3 m from the centre of the reactor (Fig. 1). The dosimeters were exposed on two polythene-bottle man phantoms filled with a $NaNO_3$ solution and at a "free air" station consisting of three thin plastic sheets for the attachment of the dosimeters.

Two irradiations were carried out on two separate days. The first run took place on April 9 with a pulse power amounting to 60.2 % of a full-size pulse (corresponding to 2.1×10^{17} fissions). The second run took place on April 14 with a pulse power amounting to 100.2 % of a full-size pulse (corresponding to 3.47×10^{17} fissions). The shielding was not altered between the two runs, so the pulses differed in size only.

During both runs the Risø dosimeters were positioned on sheet no. 5 of the "free air" station and on the front and back of phantom no. 2 (Fig. 1).

3. DOSIMETERS USED FOR THE RISØ MEASUREMENTS

The Risø measurements were carried out with the UKAEA criticality dosimeter (4,5,6) and the Risø TLD badge (7). Three criticality dosimeters and three TLD badges were irradiated in each pulse at the following respective positions: in free air, on the front of the phantom and on the back of the phantom.

The UKAEA criticality dosimeter contains two gold foils separated by a cadmium disc for the measurement of thermal and intermediate-energy neutrons, and a sulphur disc and an indium foil for the measurement of fast neutrons. The indium foil also serves as an exposure indicator in the initial phase following an accidental excursion. During the intercomparison experiment a LiF TLD 700 chip was included in each criticality dosimeter in order to provide an additional measurement of the gamma dose. This measurement is complicated by the interfering (n,γ) reactions in the gold, indium and cadmium foils in the locket. Precise corrections for this effect have not been established, so the TLDs included in the criticality dosimeters were viewed as experimental dosimeters. An exploded view of the UKAEA criticality dosimeter is shown in Fig. 2.

The composition of the Risø TLD badge is shown in Fig. 3. The TLD badge consists of an identification-coded dosimeter holder and a matching cover with photograph and name for visual identification of the employee. The dosimeter holder contains solid TL dosimeters in four depressions together with an identification number and a corresponding binary hole code. A sandwich shielding consisting of 1 mm aluminium is provided with a beta window situated so that it corresponds to one of the dosimeter positions.

For the majority of the Risø staff the dosimeter combination is two $Li_2B_4O_7$:Mn dosimeters for routine gamma and beta recording and one ^{7}LiF dosimeter to enable detection of occasional slow neutron exposures and to ensure proper interpretation of beta/gamma monitoring results by comparison of the ^{7}LiF and $Li_2B_4O_7$:Mn responses. A fourth dosimeter is reserved for readout in case of instrument failure and for verification of unusually high doses.

However, for the minority of workers, who may be exposed to neutrons, two ^{7}LiF dosimeters are used for β/γ-monitoring is order to ensure a proper β-evaluation, and an additional $Li_2B_4O_7$:Mn dosimeter is used for the detection of slow neutrons. During the intercomparison measurements at Harwell LiF TLD 700 chips (3.2 x 3.2 x 0.8 mm) were used in the TLD badge for the measurement of gamma doses.

4. MEASUREMENT PROCEDURES

The gold foils and the sulphur discs from the criticality dosimeters were counted using an end-window Geiger-Müller counter. The indium activity (fast neutron reaction) and the sodium activity were measured by the host laboratory using gamma spectrometry and all participants were provided with the results.

The TLDs were read using the TOLEDO TLD reader at Harwell. Calibrations were made with a ^{60}Co source.

5. RESULTS

5.1. Gold foils

Table I shows the fully corrected counts per minute for the gold foils and derived thermal neutron fluences (ϕ_T and ϕ_T') and intermediate-energy neutron fluences per log energy interval ($(\beta\phi_I)$ and $(\beta\phi_I)'$). The neutron fluences were derived according to the formulae given i ref. (5).

The total thermal neutron fluences incident on the free-in-air dosimeters are (from Table I):

Pulse 1: $\phi_T + \phi_T' = (2.12 + 1.91)\ 10^{10}$ n/cm^2 = $\underline{4.03 \times 10^{10}\ \text{n/cm}^2}$

Pulse 2: $\phi_T + \phi_T' = (5.05 + 8.28)\ 10^{10}$ n/cm^2 = $\underline{13.33 \times 10^{10}\ \text{n/cm}^2}$

From the measured gold-foil activities the reaction rates for gold (corresponding to infinitely thin gold foils) were derived for pulse 1 and pulse 2, respectively (6). The results are given in Table II.

5.2. Sulphur discs

The measured specific phosphorus-32 activities induced into the sulphur discs are given in the following table:

Dosimeter position		Specific ^{32}P activity dis min^{-1} g^{-1}
Pulse 1	Free air	73.1
	Phantom front	70.7 } 71.9
Pulse 2	Free air	116.3
	Phantom front	111.5 } 113.9

The average values of the specific activity (71.9 and 113.9 dis min^{-1} g^{-1} for pulse 1 and pulse 2 respectively) were used for the dose estimations. The corresponding reaction rates are given in Table II.

5.3. Indium-115m

The specific indium-115m activities measured by the host laboratory were:

Pulse 1: $X_{In} = (1.11 \pm 0.07) \times 10^4$ dis min^{-1} g^{-1}

Pulse 2: $X_{In} = (1.71 \pm 0.09) \times 10^4$ dis min^{-1} g^{-1}

5.4. Sodium

For phantom no. 2, where the Risø personnel dosimeters were positioned, the sodium activities measured by the host laboratory were:

Pulse 1: $X_{Na} = 0.942 \pm 0.014$ nCi $^{24}Na/mg\ ^{23}Na$

Pulse 2: $X_{Na} = 1.67 \pm 0.04$ nCi $^{24}Na/mg\ ^{23}Na$

From the measured thermal and intermediate-energy neutron fluences incident on the front and back of the phantom (Table I) the observed sodium activities have been corrected to give the activity (X_{Na} (F)) attributable to fast neutrons (5,6). The corrected sodium activities are

Pulse 1: X_{Na} (F) = 0.55 nCi $^{24}Na/mg\ ^{23}Na$

Pulse 2: X_{Na} (F) = 0.98 nCi $^{24}Na/mg\ ^{23}Na$

6. DOSE ESTIMATES

6.1. Recoil surface absorbed doses

The recoil surface absorbed doses were derived according to the neutron spectrum convention used for the routine evaluation of the UKAEA personnel criticality dosimeter (4,5).

According to this convention the neutron flux spectrum is assumed to be represented by the following three components:

(i) a fast neutron component represented by a Maxwellian spectrum of the form,

$$N_F(E)dE = \left(\frac{3}{\bar{E}}\right)^{\frac{3}{2}} \frac{1}{\sqrt{2\pi}} E^{\frac{1}{2}} \exp\left(-\frac{3E}{2\bar{E}}\right) dE$$

where $\bar{E}$ is the mean energy of the spectrum,

(ii) an intermediate spectrum of slowing down neutrons proportional to 1/E from 0.12 eV to 1 MeV,

$$N_I(E)dE = \frac{C}{E} \cdot dE$$

(iii) a thermal neutron component with a Maxwellian distribution of velocities appropriate to a temperature 20°C; these have a most probable energy E_T = 0.025 eV,

$$N_I(E)dE = \frac{E}{E_T^2} \exp\left(-\frac{E}{E_T}\right)dE.$$

The thermal and intermediate energy components of the recoil surface absorbed doses were derived from the incident thermal and intermediate-energy neutron fluences, respectively (cf. ref. (5)).

The fast neutron components were derived using the various methods of interpretation given in ref. 5. (Standard method for sulphur, Maxwellian method for sulphur and indium-115m, and Maxwellian method for sulphur and sodium).

The derived recoil surface absorbed doses are summarized in Table III for pulse 1 and in Table IV for pulse 2.

The large variation in the fast neutron doses calculated using the various methods of interpretation (Tables III and IV) illustrates the difficulty in measuring the neutron dose when the spectrum is rich in intermediate-energy neutrons.

The "best" neutron dose estimate is assumed to be the average of the neutron doses calculated using the Maxwellian method with sulphur and indium and with sulphur and sodium respectively, since the former method (S,In) is likely to underestimate the dose, whereas the latter method (S,Na) is likely to overestimate the dose (4).

Hence, the "best" estimates of the total recoil surface absorbed doses are:

	Dosimeter position	Recoil surface absorbed dose rads
Pulse 1	Free air	0.5(39.9 + 200.9) = 120.4
	Phantom front	0.5(38.3 + 199.3) = 118.8
Pulse 2	Free air	0.5(61.3 + 347.7) = 204.5
	Phantom front	0.5(66.6 + 353.0) = 209.8

6.2. Kerma and $^1H(n,\gamma)^2H$ surface absorbed doses

From the recoil surface absorbed dose and the average energy of the equivalent fast Maxwellian, the kerma and the $^1H(n,\gamma)^2H$ surface absorbed dose can be derived (6).

Table V shows the derived values of kerma and table VI shows the derived values of the $^1H(n,\gamma)^2H$ surface absorbed dose (based on Table XII, Fig. 4 and Fig. 5 in ref. (6)).

6.3. Gamma doses

The total TLD readings were corrected for the direct response to thermal and fast neutrons and for the influence of the TLD badge. For LiF TLD-700 a thermal-neutron sensitivity of 1.3 tissue rads per 10^{10} n/cm^2 (8,9) and a fast neutron sensitivity of 0.014 rad gamma per rad fast neutron for the VIPER spectrum (3) were assumed. In the Riso TLD badge the response of TLDs to an incident thermal-neutron fluence is enhanced mainly owing to the aluminium shielding. For LiF TLD-700 in the Riso TLD badge the equivalent response to a thermal-neutron fluence of 10^{10} n/cm^2 is 2.6 tissue rads (9).

The results of the gamma dose measurements are given i Table VII.

6.4. Summary of dose estimates

The dose estimates are summarized in Table VIII, where also the preliminary results reported during the Intercomparison Experiment at Harwell are included.

7. DISCUSSION

Before the meeting Delafield et al. (3) measured the neutron spectrum at a distance of 3 m from the VIPER reactor centre with a proton-recoil counter, a ^{3}He proportional counter and track plates. Furthermore, neutron and gamma-ray doses were measured with ionization chambers, TLDs and film dosimeters. The results of these preliminary measurements (3) are summarized in Table IX. They were disclosed to all participants in the intercomparison experiment when the participants' preliminary results from the first run had been reported.

The derived kerma spectrum for VIPER is shown in Fig. 4 (from ref. (3)). This spectrum has a mean energy of about 350 keV. In the UKAEA personnel criticality dosimeter the $^{32}S(n,p)^{32}P$ and $^{115}In\ (n,n')^{115m}In$ reactions are utilized having effective threshold energies of about 2.8 and 1.2 MeV respectively, so these reactions will detect only the few, most energetic neutrons in the upper tail of the neutron spectrum. Even the $^{237}Np(n,f)$ reaction with an effective threshold energy of about 0.75 MeV will only respond to the upper edge of the neutron spectrum, so the VIPER neutron spectrum provided a most stringent test of the participants' dosimetry systems.

The derived recoil surface absorbed doses given in Tables III and IV clearly illustrate the difficulties in measuring the neutron dose from a VIPER burst with a simple personnel dosimeter. The standard method of evaluation (with Au and S) leads to a considerable underestimation of the neutron dose (with a factor of about 5), and the Maxwellian method using Au, S and In only slightly improves this (reducing the underestimation to a factor of about 3). Hence, for a neutron spectrum rich in intermediate-energy neutrons it is essential to obtain more information than supplied by the UKAEA personnel criticality dosimeter alone. This additional information could be obtained from a neptunium or a sodium measurement (4,5,6), or from a calculation of the approximate neutron spectrum (10).

In the present work the sodium measurement (carried out by the host laboratory) was employed. This method is somewhat uncertain owing to the corrections for thermal and intermediate-energy neutrons which have to be applied (4,5,6). As described in section 6.1, the "best" neutron dose estimate was assumed to be the average of the neutron doses calculated using the Maxwellian method with S and In and with S and Na respectively, since the

former method (S,In) is likely to underestimate the dose whereas the latter (S,Na) is likely to overestimate the dose (4). This choice of an average as the final dose estimate was further supported by the resulting gamma-ray doses, since for both pulses it results in a $^{1}H(n,\gamma)^{2}H$ dose that is reasonable compared to the gamma-ray dose measured in free air and the total gamma-ray dose measured on the front of the phantom (cf. Table VIII).

The measured gamma-ray doses (Table VII) seem to be somewhat on the high side when compared to the preliminary measurements carried out by the host laboratory (3). This may indicate that the corrections for thermal and fast neutrons, and for the influence of the TLD badge, were too small. The corrections amount to 10 - 30 % of the total TL responses (Table VII). In view of the fact that corrections of this order may be necessary when using the Risø TLD badge for the measurement of gamma-ray doses in a mixed neutron/gamma radiation field, the Risø TLD badge is not ideal for nuclear accident dosimetry. A more ideal gamma-ray dosimeter would be a ^{7}LiF TL dosimeter shielded against thermal neutrons with ^{6}LiF, or a TL material less sensitive to neutrons. On the other hand, it is an administrative advantage to use the institute's standard basic personnel dosimeter for the gamma dose estimation, also in the case of accidents.

8. ACKNOWLEDGEMENTS

The author wishes to thank the IAEA, and in particular its representative F.N. Flakus, for the opportunity of participating in this intercomparison.

Furthermore it is a great pleasure to thank J.A.B. Gibson, H.J. Delafield, and all the other UK participants for their warm hospitality and kind help during the intercomparison experiment.

9. REFERENCES

(1) Weale, J.W., Goodfellow, H., McTaggart, M.H. and Warnke, E.G. The fast pulsed reactor VIPER, Part 1: General description. Journal of British Nuclear Energy Society 7, (1968) 313 - 327.

(2) McTaggart, M.H., Goodfellow, H., McCormick, W.B. and Weale, J.W. The fast pulsed reactor VIPER, Part 2: Reactor physics measurements and analysis. Journal of British Nuclear Energy Society 7, (1968), 328 - 342.

(3) Delafield, H.J. et al, Preliminary Measurements of the Uniformity of the Radiation Field and the Neutron Spectrum from the VIPER Reactor, (Unpublished).

(4) Delafield, H.J., Dennis, J.A. and Gibson, J.A.B., Nuclear Accident dosimetry; Part I, General Principles, AERE-R 7485 (1973).

(5) Delafield, H.J., Dennis, J.A. and Gibson, J.A.B., Nuclear Accident Dosimetry; Part II, Dose Assessment Procedure, AERE-R 7486 (1973)

(6) Delafield, H.J., Dennis, J.A. and Gibson, J.A.B., Nuclear Accident Dosimetry; Part III, Interpretation and Data, AERE-R 7487 (1973).

(7) Botter-Jensen, L., Christensen, P. and Majborn, B., A TLD Personnel Monitoring System with Automatic Processing Proc. of the Third International Congress of the International Radiation Protection Association, Washington, D.C., (1974), 572 - 577.

(8) Majborn, B., Botter-Jensen, L. and Christensen, P., Thermoluminescence Dosimetry applied to Areas with Mixed Neutron and Gamma Radiation Fields Proc. of the Symposium on Dosimetry Techniques applied to Agriculture, Industry, Biology and Medicine, IAEA, Vienna, (1973) 169 - 177.

(9) Botter-Jensen, L., Christensen, P. and Majborn, B., Interpretation of Monitoring Data from a Personnel TLD-badge exposed to Mixed Neutron and Gamma Radiations, Proc. of the Symposium on Neutron Monitoring for Radiation Protection Purposes, IAEA, Vienna, (1973) 261 - 272.

(10) Cross, W.G. and Ing, H., Prediction of fast neutron spectra in criticality accidents, Proc. of the Symposium on Neutron Monitoring for Radiation Protection Purposes, IAEA, Vienna, (1973) 73 - 86.

Table I.

Fully corrected counts per minute for the gold foils and derived thermal neutron fluences (ϕ_T and ϕ'_T) and intermediate-energy neutron fluences per log energy interval (($\beta\phi_I$) and ($\beta\phi_I$)').

	Criticality dosimeter no.	Dosimeter position during irradiation	Fully corrected counts per min.				Neutron fluences incident on front of dosimeter		Neutron fluences incident on back of dosimeter	
			C_a	C_b	C_c	C_d	ϕ_T 10^{10} n/cm^2	($\beta\phi_I$) 10^9 n/cm^2	ϕ'_T 10^{10} n/cm^2	($\beta\phi_I$)' 10^9 n/cm^2
PULSE 1	303520	Free air	19196	14804	13093	14771	2.12	3.84	1.91	1.73
	304193	Phantom front	27390	24080	39756	44991	4.57	3.06	10.02	4.38
	304764	Phantom back	6977	5582	7066	7733	0.93	1.21	1.59	0.62
PULSE 2	303210	Free air	34151	27294	34061	36096	5.05	5.85	8.28	1.97
	304016	Phantom front	47071	39571	62662	73587	5.33	7.10	13.26	9.51
	306752	Phantom back	12327	9621	12618	13950	1.35	2.38	2.66	1.26

Table II

Reaction rates for criticality dosimeter exposed in free air

		Reactions per 10^{10} atoms	
		PULSE 1	PULSE 2
Au-197 bare	(1)	7.84×10^{-2}	13.53×10^{-2}
	(2)	4.37×10^{-2}	10.31×10^{-2}
Au-197 in Cd	(1)	5.97×10^{-2}	9.10×10^{-2}
	(2)	2.69×10^{-2}	3.07×10^{-2}
S-32	(3)	1.13×10^{-6}	1.86×10^{-6}

NOTES

(1) An reaction rate due to neutrons incident on front of dosimeter

(2) An reaction rate due to neutrons incident on back of dosimeter

(3) Average of 8 reaction rates measured by dosimeter in free air and dosimeter on phantom front

Table III

Derived recoil surface absorbed doses.

PULSE 1.

	Method of evaluation	Thermal dose D_T rads	Intermediate dose D_I rads	Fast dose rads	Total recoil dose rads	Average energy of equivalent fast Maxwellian MeV
Free air	Standard (Au,S)	1.2	15.6	6.0	22.8	1.96
	Maxwellian (Au,S,In)	1.2	15.6	23.1	39.9	0.98
	Maxwellian (Au,S,Na)	1.2	15.6	184.1	200.9	0.54
Phantom front	Standard (Au,S)	2.7	12.5	6.0	21.2	1.96
	Maxwellian (Au,S,In)	2.7	12.5	23.1	38.3	0.98
	Maxwellian (Au,S,Na)	2.7	12.5	184.1	199.3	0.54

Table IV.

Derived recoil surface absorbed doses.

PULSE 2.

	Method of evaluation	Thermal dose D_T rads	Intermediate dose D_I rads	Fast dose rads	Total recoil dose rads	Average energy of equivalent fast Maxwellian MeV
Free air	Standard (Au,S)	2.9	23.8	9.5	36.2	1.96
	Maxwellian (Au,S,In)	2.9	23.8	34.6	61.3	1.00
	Maxwellian (Au,S,Na)	2.9	23.8	321.0	347.7	0.53
Phantom front	Standard (Au,S)	3.1	28.9	9.5	41.5	1.96
	Maxwellian (Au,S,In)	3.1	28.9	34.6	66.6	1.00
	Maxwellian (Au,S,Na)	3.1	28.9	321.0	353.0	0.53

Table V.

Contribution to kerma from thermal, intermediate-energy and fast neutrons and the resulting total kerma.

	Dosimeter position	Detectors	Thermal Contribution rads	Intermediate Contribution rads	Fast Contribution rads	Total kerma rads	Average total kerma rads
PULSE 1	Free air	Au,S,In	0.4	15.4	21.5	37.3	92.1
		Au,S,Na	0.4	15.4	191.1	206.9	
	Phantom front	Au,S,In	0.9	12.3	21.5	34.7	119.5
		Au,S,Na	0.9	12.3	191.1	204.3	
PULSE 2	Free air	Au,S,In	1.0	23.4	32.1	56.5	207.4
		Au,S,Na	1.0	23.4	333.8	358.2	
	Phantom front	Au,S,In	1.1	28.5	32.1	61.7	212.6
		Au,S,Na	1.1	28.5	333.8	363.4	

Table VI.

Contributions to $^{1}H(n,\gamma)^{2}H$ surface absorbed dose from thermal, intermediate-energy and fast neutrons and the resulting total $^{1}H(n,\gamma)^{2}H$ surface absorbed dose.

	Dosimeter position	Detectors	Thermal Contribution rads	Intermediate Contribution rads	Fast Contribution rads	Total $^{1}H(n,\gamma)^{2}H$ dose rads	Average total $^{1}H(n,\gamma)^{2}H$ dose rads
PULSE 1	Free air	Au,S,In	8.3	24.2	2.7	35.2	50.9
		Au,S,Na	8.3	24.2	34.1	66.6	
	Phantom front	Au,S,In	18.6	19.4	2.7	40.7	56.4
		Au,S,Na	18.6	19.4	34.1	72.1	
PULSE 2	Free air	Au,S,In	20.0	36.9	3.9	60.8	89.0
		Au,S,Na	20.0	36.9	60.3	117.2	
	Phantom front	Au,S,In	21.4	44.8	3.9	70.1	98.3
		Au,S,Na	21.4	44.8	60.3	126.5	

TABLE VII

Gamma doses measured with LiF TLD-700

	Dosimeter position	Total TL response eq. rads	Correction for thermal neutrons eq. rads	Correction for fast neutrons eq. rads	γ dose rads
Pulse 1	Free air	74.4	10.5	1.5	62.4
	Phantom front	152.3	37.9	1.5	112.9
	Phantom back	66.6	6.6	0	60.0
Pulse 2	Free air	125.1	34.7	2.5	87.9
	Phantom front	245.3	48.3	2.5	194.5
	Phantom back	105.6	10.4	0	95.2

TABLE VIII

Summary of dose estimates

	Dosimeter position	Kerma rads	Surface absorbed neutron dose: Recoil rads	Surface absorbed neutron dose: $^{1}H(n,\gamma)^{2}H$ rads	Gamma dose rads
Pulse 1	Free air (preliminary results/10.4.75)	122 (128)	120 (125)	51 (54)	62 (65)
	Phantom front (preliminary results/10.4.75)	120 (124)	119 (122)	56 (57)	113 (116)
Pulse 2	Free air (preliminary results/15.4.75)	207 (209)	205 (204)	89 (90)	88 (86)
	Phantom front (preliminary results/15.4.75)	213 (216)	210 (210)	98 (100)	195 (192)

Table IX

Summary of preliminary U.K. measurements for full size pulse from VIPER reactor. The table is based on Table VII in ref (3).

Measurement	Data	Method
Free air (3 m from centre of reactor)		
Neutron kerma (rad)	215 211	Measured spectrum CH ionisation chamber/ TLD/Film
Incident gamma-ray dose (rad)	73	TLD/Film
Neutron fluence (10^{10} ncm^{-2}) Thermal(1)	6.7	Gold foil pack
>0.1 eV	28.3	Measured spectrum
>1 keV	27.2	- -
>0.75 MeV	1.5	- -
>1.5 MeV	0.36	- -
>2.5 MeV	0.11	- -
Surface absorbed dose to front of phantom (2.91 m from centre of reactor)		
Neutron dose (recoil + proton) (rad)	202	Measured spectrum
$^{1}H(n,\gamma)^{2}H$ dose (rad)	110	Measured spectrum
Total gamma-ray dose (rad)	160	TLD/Film

Notes (1) Sum of thermal fluences incident on front and back of dosimeter

(2) Doses derived from the measured spectrum include a small additional correction for thermal neutrons

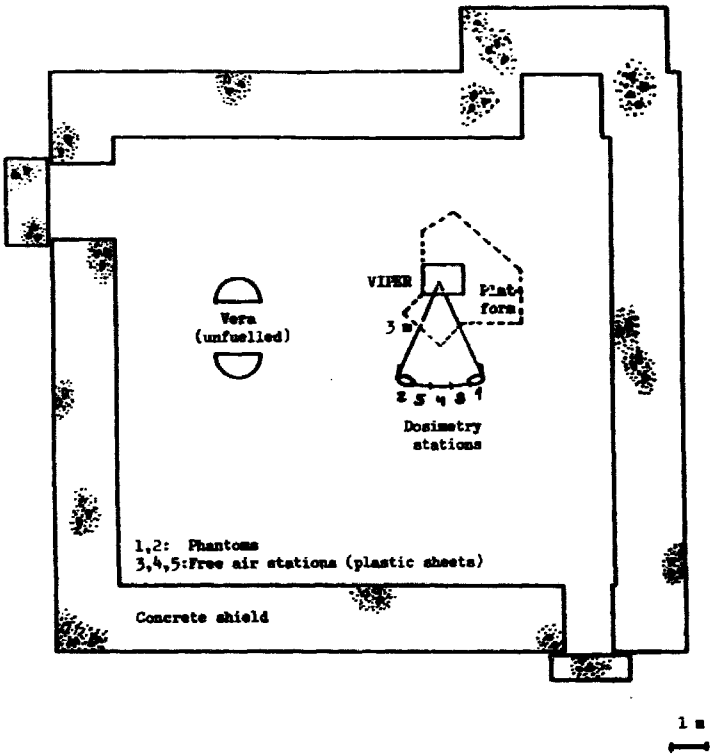

Fig. 1 Exposure arrangement in the VIPER reactor cell. At both pulses the Riso dosimeters were positioned on free air station no. 5 and on the front and back of phantom no. 2. (based on Fig. 2 in ref. (3)).

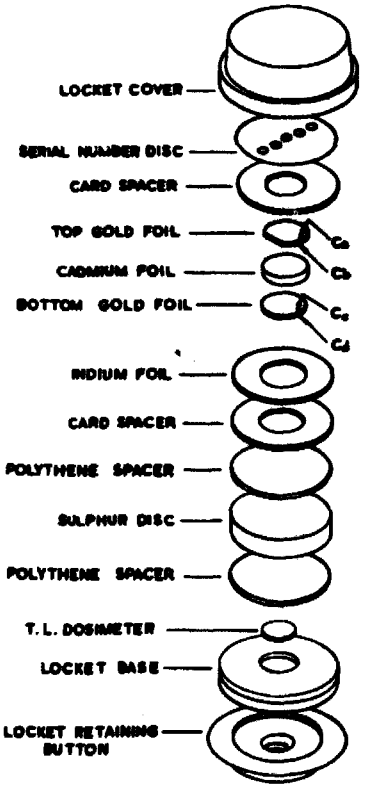

Fig. 2. Exploded view of UKAEA personnel criticality dosimeter (from ref. (4)).

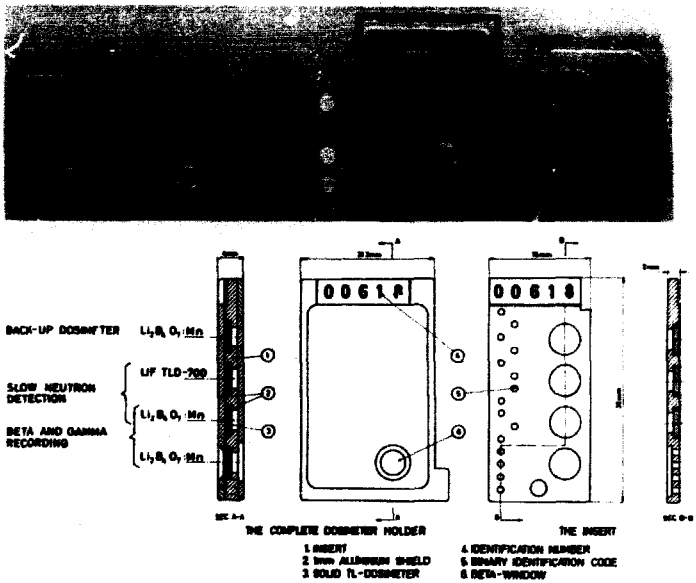

Fig. 3. The Risø TLD badge. At the top: an exploded view of the entire TLD badge, and at the bottom: a schematic diagram of the TLD holder. The dosimeter combination shown is that which is used for the majority of the workers at Risø. However, for workers who may be exposed to neutrons, two LiF TLD 700 dosimeters are used for β/γ-monitoring. At the intercomparison experiment at Harwell LiF TLD 700 was used for the measurement of gamma-ray doses.

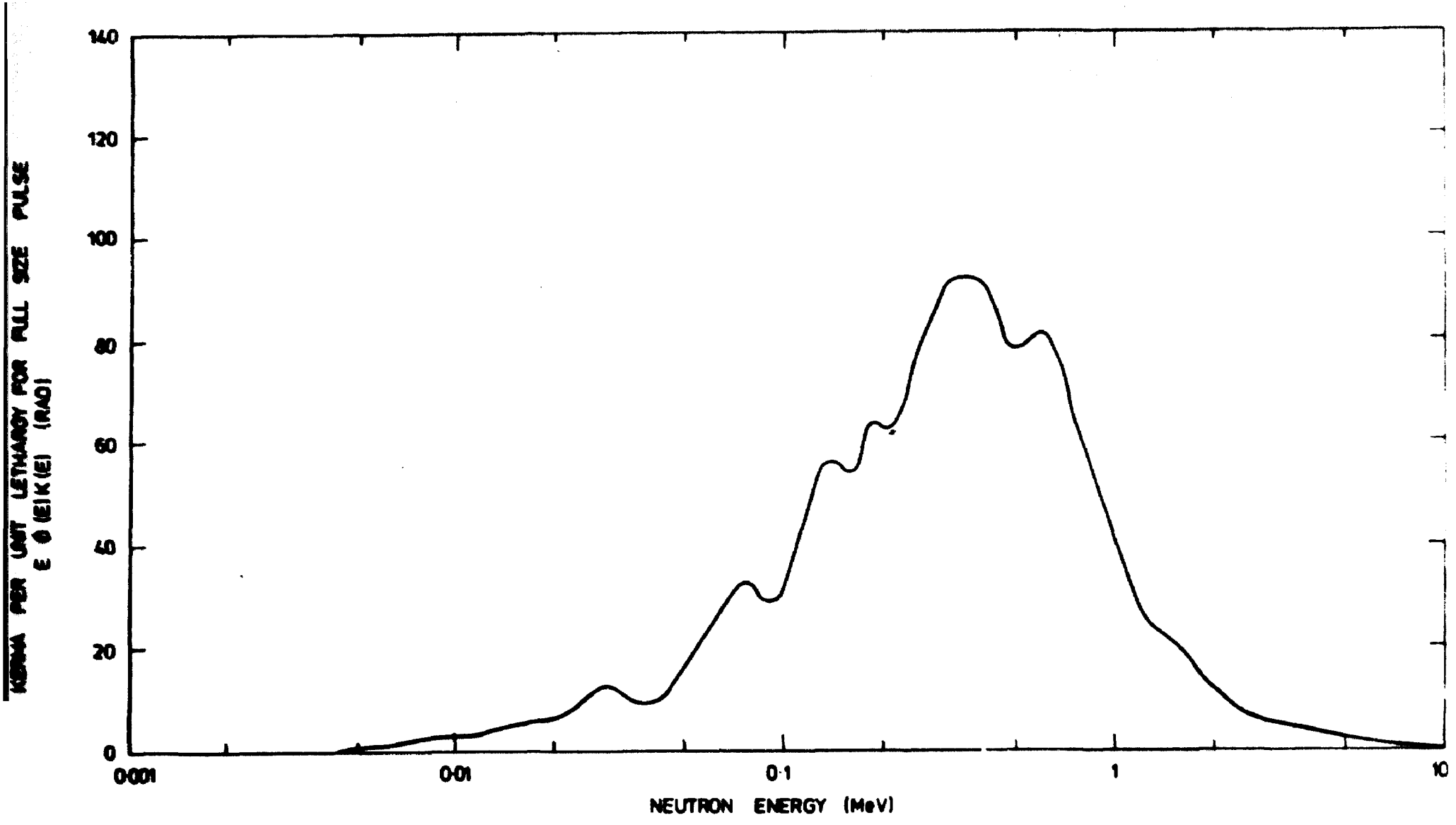

Fig. 4. Derived neutron kerma spectrum at 3 m from the centre of the VIPER reactor core (from ref. (3)).